Journal of
Computational and Theoretical Nanoscience
Vol. 8, 1–6, 2011

Energy Dissipation of Nanoporous MFI Zeolite Under Dynamic Crushing

Baoxing Xu[1,†], Ling Liu[1,†], Yu Qiao[2,3], Mooho Tak[4], Taehyo Park[4], and Xi Chen[1,4,5,*]

[1] *Columbia Nanomechanics Research Center, Department of Earth and Environmental Engineering, Columbia University, New York, NY 10027, USA*
[2] *Department of Structural Engineering, University of California – San Diego, La Jolla, CA 92093-0085, USA*
[3] *Program of Materials Science and Technology, University of California – San Diego, La Jolla, CA 92093-0085, USA*
[4] *Department of Civil and Environmental Engineering, Hanyang University, Seoul, 133-791, Korea*
[5] *School of Aerospace, Xi'an Jiaotong University, Xi'an 710049, China*

Nanoporous materials are emerging as a potential candidate for high-performance energy dissipation. Understanding the mechanical response upon crushing is important for designing nanoporous material structures with maximum energy dissipation. Using molecular dynamics simulations, we investigate the crushing behaviors of a MFI zeolite upon different loading rates, compression directions, and with different sample thickness. The dissipation mechanism is expected to result from the non-uniform collapse of nanopores and the spread of the thus formed densification region through the structure. The results show that the loading along the tortuous nanopore path ([001]-orientation) may maximize the energy dissipation. Strong loading rate effect is observed which couples with orientation dependence, yet the effect of thickness is relatively minor.

Keywords: Energy Dissipation, Nanoporous Material, Molecular Dynamics Simulation.

RESEARCH ARTICLE

1. INTRODUCTION

Energy dissipation plays a crucial role for the safety and integrity of materials and structures subjected to dynamic loadings.[1–3] Inspired by natural materials and structures, energy dissipation/absorption materials with micro or nanoporous structures are attracting growing interests.[4,5] Kyriakides et al. have systematically studied the energy absorption mechanism of honeycomb structures.[6,7] and porous materials,[8,9] and found that upon external loading, the porous structure usually experiences cell shear slip, buckling, and crushing, through which a large amount of energy is dissipated via large and widespread permanent deformation; the same principles apply when the pore size is of micron level.[10] For nanoporous materials, Han et al.[11] found that the energy dissipation efficiency of a nanoporous silica gel is on the order of 300 J/g (when the applied quasi-static compressive strain is only about 4%), which is much higher than most conventional protection and damping materials thanks to the small pore size, high porosity, and high network strength. Despite of the promising performance potential demonstrated in the preliminary experiment,[11] it remains unclear whether the energy dissipation mechanism of nanoporous material is similar to that of larger pores, due to the intriguing size effects that are often observed at the nanoscale.

With its sub-nm pore size, high specific surface area, and highly regular and uniform pore structure, MFI zeolite is considered as a promising candidate for energy absorption and dissipation system.[12,13] Inside a MFI zeolite, two channel systems co-exist:[14] zigzag channels along the direction of the *a*-axis ([100]) interconnected with straight channels along *b*-axis ([010]). A tortuous pore path is presented along the *c*-axis. Figure 1 shows the internal pore structure of MFI zeolite from different directions. When subjected to an external loading, although one expects that the crushing deformation of nanopores can dissipate a large amount of energy, the ultra-small pore size, variation of pore alignments with respect to different loading directions, and the interconnected pore structure may significantly affect the energy dissipation process, which need to be revealed from detailed atomistic simulations. In the

*Author to whom correspondence should be addressed.
† These authors contributed equally to this work.

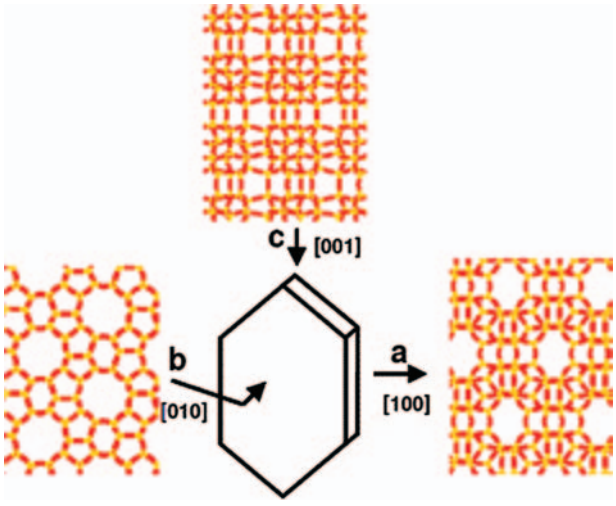

Fig. 1. MFI zeolite atomic structures and the views from the three loading directions in this paper.

present study, the dynamic response of nanoporous MFI zeolite at constant loading rates is simulated using molecular dynamic (MD) approach, and the pore deformation mechanism under compressive loading and energy dissipation principles are revealed. The loading direction, loading rate, and sample thickness are also varied to explore their effects. A possible pore alignment along which maximum energy dissipation may be obtained is suggested.

2. MODEL AND COMPUTATIONAL METHOD

With the aforementioned internal channel alignments, the mechanical property of MFI zeolite is anisotropic and we examine its crushing response along [100], [010] and [001] loading directions. The cell parameters after optimization are $a = 18.1286$ Å, $b = 20.4136$ Å and $c = 14.5949$ Å in the [100], [010] and [001]-orientations respectively, and $\alpha = \beta = \gamma = 90^0$. For a given loading direction, such as [100], a number of cells are stacked along this direction to reach a specific thickness, and periodic boundary conditions are imposed in the four lateral directions, to simulate the compression of a zeolite thin film (along [100] direction in this example); the film thickness (t) in the loading direction is varied to explore its effect. The bottom of the film is held fixed and the loading is applied through a moving rigid plane (with a controlled displacement rate) on the top surface of the film, where the compressing pressure is computed as a function of applied compressive strain; the loading rate is also varied to study its effect.

MD simulations are carried out by using Materials Studio.[15] The force field COMPASS (Condensed-phase Optimized Molecular Potentials for Atomistic Simulation Studies[16]) is used to model the atomic interactions. The summation methods for both van der Waals and Coulomb forces are atom based with cutoff, spline width and buffer width of 10, 1.0 and 0.5, respectively. Simulation temperature is set to 300 K and the controlling method is Berendsen method with the Decay constant of 0.1.

3. RESULTS AND DISCUSSION

3.1. Loading Rate-Dependence of Crushing Deformation

The typical pressure–strain curves of MFI zeolite in response to crushing are shown in Figure 2(a), where loading is applied along the [001] direction and the undeformed film thickness (t) is 16.05 nm. A linear variation of pressure with the applied compressive strain is observed at the initially loading stage, which is essentially independent on the loading rate, thus indicating uniform elastic deformation of the nanoporous structure (i.e., the Young's modulus measured from the crushing curve is essentially

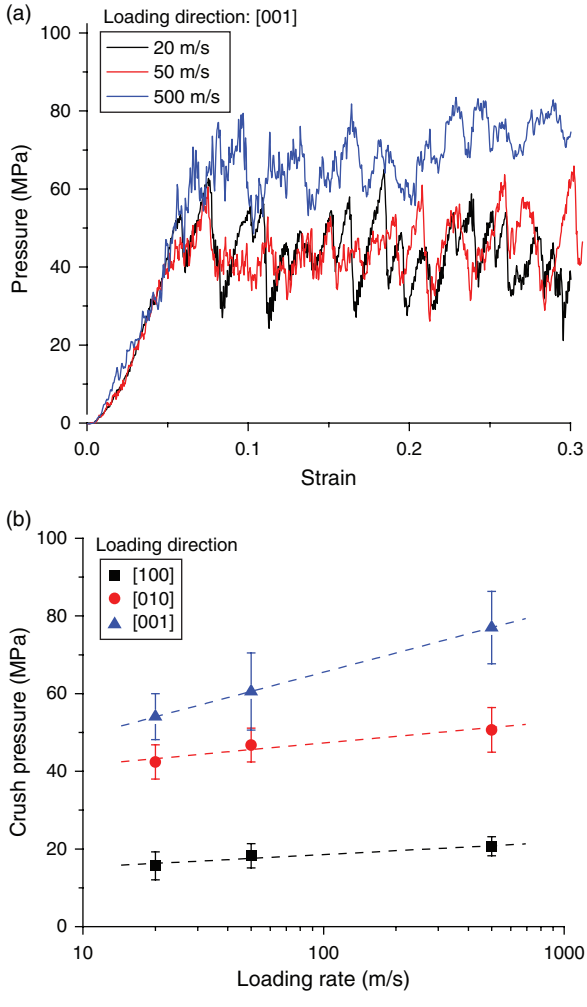

Fig. 2. (a) Representative pressure–strain curves of MFI zeolite subjected to compressive (crush) loading along the [001]-orientation with several different loading rates; the undeformed zeolite thickness (t) is 16.05 nm along [001] direction. (b) Effect of the loading rate on the critical crushing pressure for loading along different orientations.

RESEARCH ARTICLE

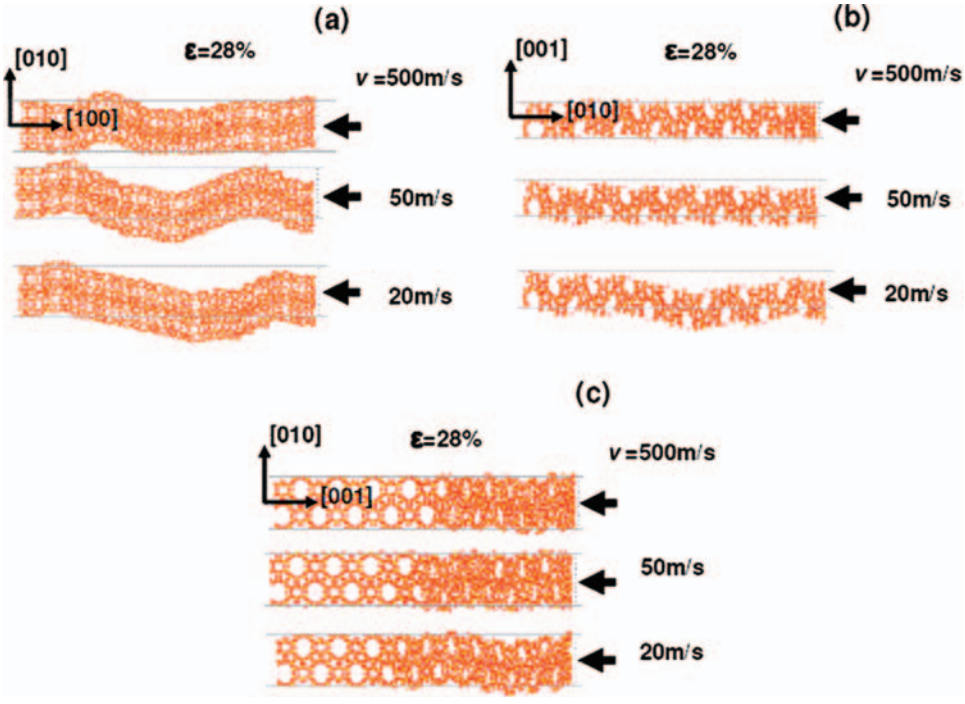

Fig. 3. Deformed pore structure of MFI zeolite unit cell (the periodic boundary condition is imposed on all 4 lateral surfaces; the undeformed zeolite thickness is about 16.05 nm for all three orientations), at the compressive strain of 28% with loading rate of 500, 50 and 20 m/s; the loading is applied along (a) [100]-orientation; (b) [010]-orientation; (c) [001]-orientation.

independent of the loading rate). As the strain is increased, the pressure shows an undulation behavior which is associated with the local sequential and permanent collapse of the nanopores (see below for configuration evolution of the nanopores), qualitatively similar to what have been observed in larger scale honeycombs.[6, 7] (note that unlike the uniformly aligned honeycombs in Refs. [6, 7], in this study there are two nanochannel systems interconnected together.)

The structural deformation shows a rate-dependent behavior in the permanent "plastic" deformation stage, which should be again attributed to the nanoscopic channel collapse characteristics in response to different loading rates (by contrast, in nonporous materials the loading rate dependent properties are usually due to dislocation movements, and depends on both grain size and crystal structure[17, 18]). Similarly to the crushing behavior of large scale honeycombs, we define the maximum pressure of the initial linear elastic stage (at the onset of the permanent pore collapse followed by the undulations of pressure) as the critical crushing pressure. It can be seen from Figure 2(a) that both the critical crushing pressure and mean undulation pressure increase with the increase of the loading rate, and such a rate effect is qualitatively similar to the response of the larger scale honeycomb.[6, 7] Figure 2(b) further examines such a rate-dependent behavior at different loading directions. The most prominent loading rate effect is observed along the [001]-orientation. In other words, the rate-dependence of MFI zeolite crushing behavior is also a function of the pore configuration/alignment. For zigzag and straight nanochannels (aligned in [100]- and [010]- directions), although both them consist 10-member-rings, they show different loading rate sensitivities and this difference is expected to results from the nanochannel geometric pattern/alignment. In addition, the straight channels are more buckling resistant than the zigzag ones, which will be discussed in more detail in the next subsection. Whereas along the [001] loading direction, the tortuous nanochannels are "mixed" and as a consequence of the interaction between straight and zigzag channels, the [001] direction seem to have higher collapse pressure as well as showing the highest loading rate dependence. For all orientations, just like the larger scale honeycombs,[6, 7] any imperfection inside the porous structure is expected to enhance the rate-dependence of pore collapse.

Figure 3 shows the deformation characteristics at the strain of 28% under three loading rates. The comparisons show that if the loading rate is high, the collapse is more concentrated near the surface of the film (where the load is applied), and the formation of such a densification region requires a larger pressure.[a] Whereas

[a]During the loading process with high loading rate, if the rigid plane is stopped and its position is fixed, the pressure (as well as the atomic structure) will moderately relax; this is not observed in the slower loading rates in this study.

RESEARCH ARTICLE

for lower loading rates, since there is more time for the structure to optimize its configuration, the collapse is more widespread yet the relative closing of the pore is not as extensive as that at the higher rate, resulting in a lower pressure and strain energy; in addition, with the increase of compressive strain, the layers of pores tend to undergo shear slip in the lateral direction (instead of further collapsing the pores), similar to that have been observed for large scale honeycombs at low strain rates.[6, 7]

3.2. Orientation-Dependence of Crushing Deformation

Figure 4 shows the effect of different loading directions (along [100], [010] and [001] orientations) on the pressure–strain curves with a representative loading rate of 50 m/s. All of them show similar behaviors: an initial linear elastic deformation stage followed by a long undulation stage governed by permanent pore sequential collapse (which dissipates a large amount of energy). From the linear elastic range, the Young's modulus of 1.6 ± 0.1 GPa can be extracted along the [100]- and [010]-directions, which is on the same order a previous quasi-static compression experiment,[19] and indicates that the elastic anisotropy at [100]- and [010]- orientations are weak. Meanwhile, the Young's modulus along the [001]-orientation is 0.9 ± 0.05 GPa, more compliant than the other two orthogonal directions.

The pore collapse behavior is quite anisotropic owing to the different pore alignments with respect to the loading directions (unlike that in nonporous materials whose anisotropic behaviors are caused by slip planes[20]). For [100] direction, a continuously increasing pressure is required in order to collapse more zigzag pores (although the critical crushing pressure is low). For [010] and [100] directions, the critical crushing pressure is higher (especially for the [001] direction due to the interaction of zigzag and straight nanochannels), yet one does not to increase the pressure much to sustain the sequential pore collapses. The dissipated energy can be determined from the area bounded by the pressure–strain curve, the extent of which also depends on the applied compressive strain (assuming it is not affected by fracture). At a compressive strain of 28% and loading rate of 50 m/s, the potential energy dissipation efficiency is about 1.58, 2.01 and 2.08 KJ/g, respectively for [100]-, [010]- and [001]-orientations, comparable with experimental result if the strain level is similar.[11, b] When the loading rate is higher at 500 m/s, the energy dissipation is larger due to the aforementioned rate effect, and the results are 2.14, 2.81 and 3.06 KJ/g, respectively for [100]-, [010]- and [001]-orientations; at a lower loading rate of 20 m/s, the energy dissipation is 1.42, 1.89 and 2.06 KJ/g, respectively for the three directions. These values are significantly higher than that of conventional energy dissipation materials such as composites or shape memory alloys,[1] as well as better than that of nanoporous material functionalized (NMF) liquids such as silica gel immersed in an aqueous solution of electrolyte.[21–24] For all loading rates examined, the MFI zeolite can absorb maximum amount of energy if the compression is applied along the [001]-direction, which can be attributed to the advantageous nanopore collapse mechanism (compare with other two directions), analyzed below.

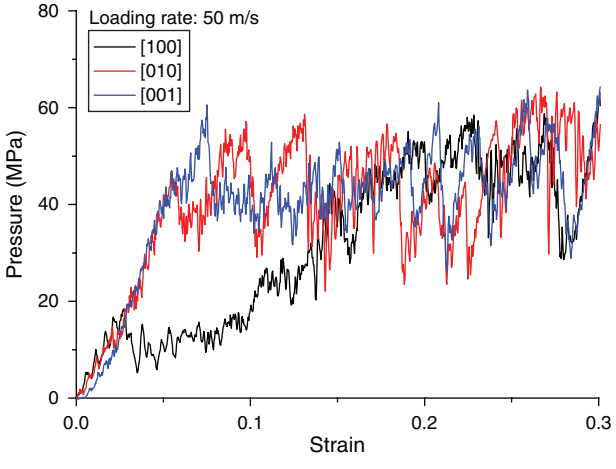

Fig. 4. Effect of the loading direction on the pressure–strain crush curves of MFI zeolite at the loading rate of 50 m/s. All zeolite sample thicknesses are about 16.05 nm.

Figure 5 shows the deformed nanostructure characteristics at the strain of 9.3% and 28%, respectively. For [100] loading direction, at a higher strain (28%), lateral shear slip between layers of pores is developed, which is consistent with the oscillation in pressure magnitude in Figure 4. In contrast, a densification region is found near the top surface of film (where the external crushing load is applied) for [010]- and [001]- orientations at small strain; the densification seems to be higher for the [001]- loading than [010] loading. With increased strain level, both [010]- and [001]- loading cases show sequential propagation of pore collapse at almost constant pressure level (although the buckle behaviors are different for different pore orientations), which is the main mechanism for energy absorption; since the pore collapse and densification are non-uniform, the required pressure increases a little bit at higher strain.

Although the orientation-dependence results in this section are specified for 50 m/s loading rate, same mechanism and findings hold for the other loading rates investigated. The orientation-dependent crushing behavior suggests that the zigzag channels ([100]- orientation) are the most unstable and upon compression, they undergo shear slip, whereas the interconnected straight and zigzag

[b]The unloading behavior is almost linear with a slope close to that of initial loading stage, and the recovery of elastic energy is very small. The energy absorbed/dissipated is calculated by integrating the pressure–strain curve in Figure 4.

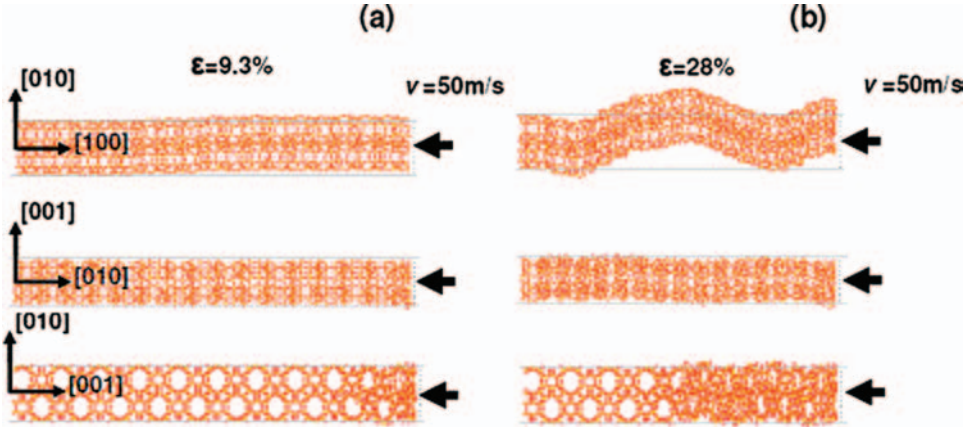

Fig. 5. Deformed pore structure of MFI zeolite unit cell subjected to loading along three different orientations (their crushing curves in Fig. 4). The compressive strain is (a) 9.3% and (b) 28%. The loading rate is 50 m/s, and all sample thicknesses is about 16.05 nm.

channels facing the [001] direction can be more collapse resistant (which leads to non-uniform pore collapse with enhanced loading rate effect in Fig. 2). In other words, a larger energy dissipation performance can be obtained if the non-uniform pore collapse mechanism dominates over lateral shear slip. This is consistent with the energy absorption performance of experiment on nanoporous silica gels,[11] and numerical simulation on honeycombs.[25]

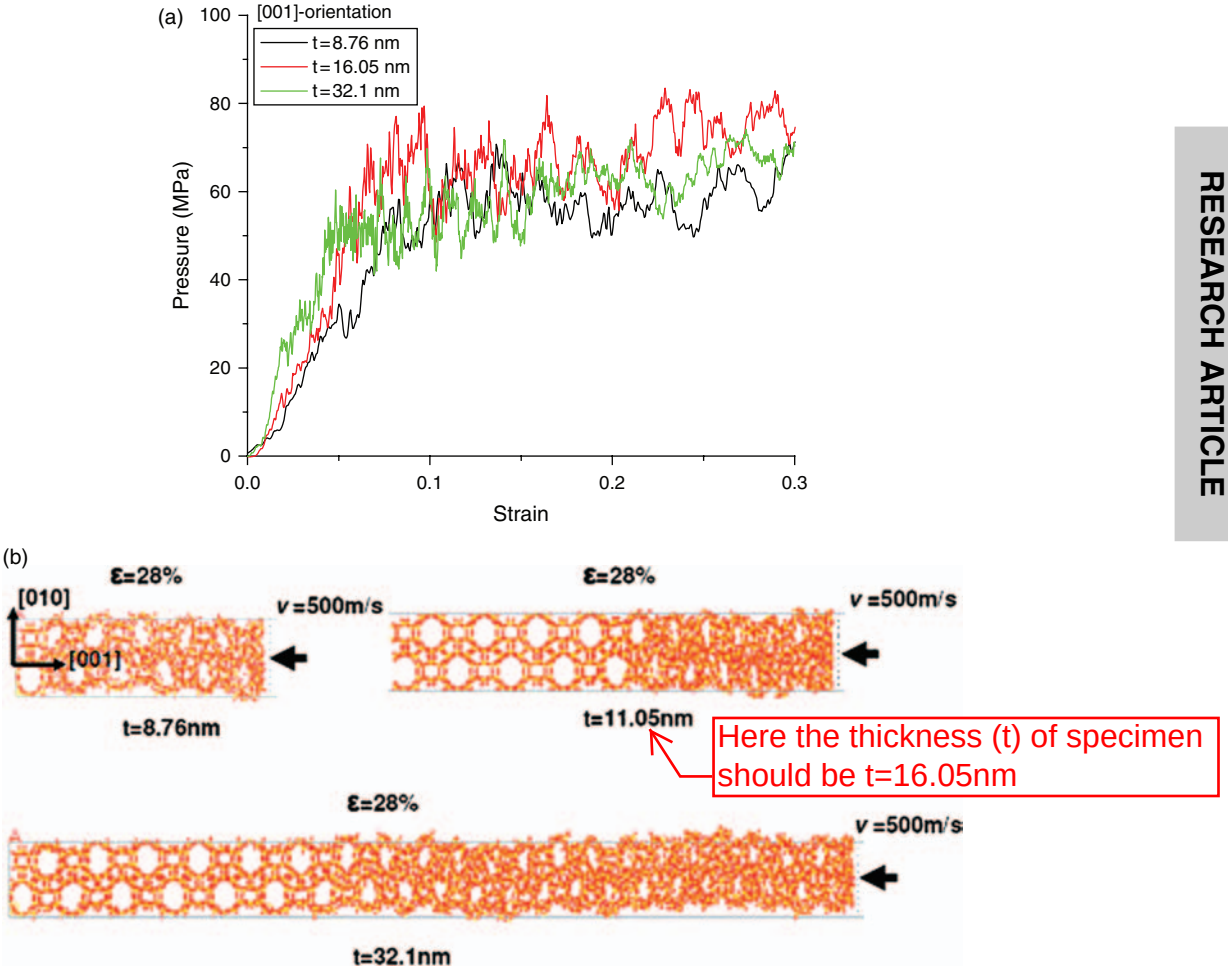

Fig. 6. Deformed pore structure of MFI zeolite subjected to loading along [001] orientation. (a) Compressive load–strain curve; (b) Crushed structures under stain of 28% for three different thickness. The loading rate is 500 m/s.

3.3. Size-Dependence of Crushing Deformation

Figure 6 shows the effect of specimen size (thickness) on the crushing curve, where the load is applied along the [001]-orientation with a loading rate of 500 m/s (similar thickness dependences are found for other loading rates studied); the thickness (t) of the 3 specimens in Figure 6 are 8.76 nm, 16.05 nm, and 32.1 nm, respectively. A slight increase of the slope of the initial elastic stage is observed for the larger specimen in Figure 6(a) while other main features such as the critical crushing pressure and energy absorption remain close. Figure 6(b) shows the crushed structures under a compressive strain of 28% for three different specimen thicknesses, and almost the same deformation patterns are observed, which echoes the crushing curve in Figure 6(a). Therefore, the effect of specimen size on the crushing deformation/energy dissipation is not very prominent, and is similar with the conventional large scale honeycombs[6,7] and nano scale honeycombs.[26]

4. CONCLUDING REMARKS

The dynamic responses of a MFI zeolite under various loading rates and loading directions are investigated by using molecular dynamics simulations. During the elastic deformation stage at very small strain, the response shows weak anisotropy along the [100]- and [010]- directions, and the stiffness is much smaller in the [001] direction. Above the critical crushing pressure, the permanent and sequential pore collapse behaviors are highly anisotropic and loading rate dependent (some characteristics are qualitatively similar to the crush of honeycombs, although the pore structure of zeolite is much more complex); the orientation and loading rate effects are coupled. If the load is applied along the [100]-orientation, the nanopore collapse mechanism is dominated by the lateral shear slip deformation during the permanent deformation stage. For loading along the [001] direction, due to the interaction of zigzag and straight nanochannels, the structure is more crush resistant (and thus having higher potential for energy dissipation) and the loading rate effect is also the most prominent; the crushing is dominated by the spread of densification region of the collapsed pores through the structure (also for [010] direction). The results may shed some light on the optimal design of energy dissipater and absorbers using nanoporous materials.

Acknowledgment: The work is supported by the National Science Foundation (NSF) under grant number CMMI-0643726, a World Class University (WCU) program through the National Research Foundation of Korea funded by the Ministry of Education, Science and Technology of Korea (R32-2008-000-20042-0), and by National Natural Science Foundation of China Grant No. 50928601.

References

1. G. Lu and T. Yu, Energy Absorption of Structures and Materials, CRC Press, Hong Kong **(2003)**.
2. L. Sun, R. F. Gibson, F. Gordaninejad, and J. Suhr, *Compos. Sci. Technol.* 69, 2392 **(2009)**.
3. L. J. Gibson and M. F. Ashby, Cellular Solids: Structure and Properties, Cambridge University Press, Cambridge **(1997)**.
4. N. Kroger and K. H. Sandhage, *MRS Bull.* 35, 122 **(2010)**.
5. K. Tai, M. Dao, S. Suresh, A. Palazoglu, and C. Ortiz, *Nat. Mater.* 6, 454 **(2007)**.
6. S. D. Papka and S. Kyriakides, *Int. J. Solids Structures* 35, 239 **(1997)**.
7. S. D. Papka and S. Kyriakides, *Acta Mater.* 46, 2765 **(1998)**.
8. L. Gong, S. Kyriakides, and N. Triantafyllidis, *Journal of the Mechanics and Physics of solids* 53, 771 **(2005)**.
9. L. Gong and S. Kyriakides, *Journal of Applied Mechanics* 73 **(2006)**.
10. W. Y. Jang, A. M. Kraynik, and S. Kyriakides, *International Journal of Solids and Structures* 45, 1845 **(2008)**.
11. A. Han, V. K. Punyamurthula, W. Lu, and Y. Qiao, *J. Appl. Phys.* 103, 084318 **(2008)**.
12. V. Eroshenko, R.-C. Regis, M. Soulard, and J. Patarin, *J. Am. Chem. Soc.* 123, 8129 **(2001)**.
13. Y. Qiao, L. Liu, and X. Chen, *Nano Lett.* 9, 984 **(2009)**.
14. I. Dı'az, E. Kokkoli, O. Terasaki, and M. Tsapatsis, *Chem. Mater* 16, 5226 **(2004)**.
15. MaterialsStudio, Materials Studio 4.0 User's Manual Accelrys Software Inc., San Diego, California **(2005)**.
16. H. Sun, P. Ren, and J. R. Fried, *Comput. Theor. Polym. Sci.* 8, 229 **(1998)**.
17. D. Caillard and J. L. Martin, Thermally Activated Mechanisms in Crystal Plasticity, Pergamon, Amsterdam **(2003)**.
18. M. Dao, L. Lu, Y. F. Shen, and S. Suresh, *Acta Mater.* 54, 5421 **(2006)**.
19. Z. Wang, J. Lambros, and R. Lobo, *J. Mater. Sci.* 37, 2491 **(2002)**.
20. F. A. McClintock and A. S. Argon, Mechanical Behavior of Materials, Addison-Wesley, Reading, Massachusetts **(1966)**.
21. X. Chen, F. B. Surani, X. Kong, V. K. Punyamurtula, and Y. Qiao, *Appl. Phys. Lett.* 89, 241918 **(2006)**.
22. J. Zhao, P. J. Culligan, J. T. Germaine, and X. Chen, *Langmuir* 25, 12687 **(2009)**.
23. L. Liu, Y. Qiao, and X. Chen, *Appl. Phys. Lett.* 92, 101927 **(2008)**.
24. X. Chen, G. Cao, A. Han, V. K. Punyamurtula, L. Liu, P. J. Culligan, T. Kim, and Y. Qiao, *Nano Lett.* 8, 2988 **(2008)**.
25. D. Karagiozova and T. X. Yu, *International Journal of Mechanical Sciences* 47, 570 **(2005)**.
26. D. Choi, J. Jeon, P. Lee, W. Hwang, K. Lee, and H. Park, *Compos. Struct.* 79, 548 **(2007)**.

Received: 27 March 2010. Accepted: 4 May 2010.